

2013

Effects of a BMP antagonist on fracture healing in a mouse model

<https://hdl.handle.net/2144/12165>

"Downloaded from OpenBU. Boston University's institutional repository."

BOSTON UNIVERSITY
SCHOOL OF MEDICINE

Thesis

**EFFECTS OF A BMP ANTAGONIST ON FRACTURE HEALING IN A MOUSE
MODEL**

by

ALEXANDER KIM MOUNTS

B.S., College of William & Mary, 2011

Submitted in partial fulfillment of the
requirements for the degree of
Master of Arts

2013

Approved by

First Reader

Louis C. Gerstenfeld, Ph.D.
Director of Orthopaedic Research Laboratory
Professor of Orthopaedic Surgery
Research Professor of Biochemistry

Second Reader

Anthony DeGiacomo, M.D.
Orthopaedic Research Fellow

ACKNOWLEDGEMENTS

I would first like to thank Dr. Gerstenfeld for accepting me into his lab, teaching me so much, and for the invaluable experience I've gotten while working in his lab. A special thanks to Dr. Anthony DeGiacomo for letting me work with him on this project and for everything he taught me while working with him. Thank you to Gabriel McDonald for all the help learning to use the microCT machine and for the enormous amount of time he put in to help me.

EFFECTS OF A BMP ANTAGONIST ON FRACTURE HEALING IN A MOUSE MODEL

ALEXANDER KIM MOUNTS

Boston University School of Medicine, 2013

Major Professor: Louis C. Gerstenfeld, Ph.D., Professor of Orthopaedic Surgery,
Research Professor of Biochemistry

ABSTRACT

Introduction: Fracture healing is a complex process that is responsible for forming a fracture callus to stabilize the site of injury while producing new bone. Delayed fracture healing or the development of non-union as a result of failed fracture healing is a major clinical concern effecting ~10% of all treated fractures. Recent studies have shown that RAP-661, an antagonist of Bone Morphogenetic Proteins (BMP) 2 and BMP-4 binding to its receptor BMPR-1A has shown anabolic efficacy in treating bone loss associated with osteoporosis. The purpose of this study was to assess the effectiveness of the RAP-661 protein as a therapeutic agent to improve fracture healing.

Materials and Methods: 34 C57/B6 mice received unilateral mid-shaft transverse right femur fractures. Three study groups used: Vehicle Treated Control (10 mM Tris-Buffered Saline) and RAP-661 in 10 mM TBS either where

the drug treatment was administered continuously over the 35 days of the study or administered with a delayed treatment beginning 14 day after fracture. Both drug and vehicle were administered via intraperitoneal injection twice per week. RAP-661 was administered at 10 mg/kg for each injection. The mice were terminally harvested at 35 days. The harvested femora were then tested via microCT analysis for material and structural properties and by mechanical testing for strength and torsional stiffness and rigidity.

Results: MicroCT testing showed that both drug groups had increased bone volume and bone volume percentage. Mechanical testing however, showed that the control group was significantly stronger based on its maximal torque to failure than both either drug treatment group. Although not significant, the 35 day delay group showed comparable stiffness and rigidity to the control and trended toward higher values compared to the 35 day continuous group.

Conclusion: Although both drugs groups had increased total mineral density and percentage bone volume, they both had significantly lower maximal torque to failure when compared to the control. This discordance indicates that while the RAP-661 improves overall bone accumulation, it is effecting the structural integrity of bone bridging in some manner that compromise the regain of the bone's normal mechanical strength. Further research will be needed to resolve the mechanism(s) behind this phenomenon. These results indicate that RAP-661 does not show therapeutic efficacy in promoting fracture healing.

TABLE OF CONTENTS

Title		i
Reader's Approval Page		ii
Acknowledgements		iii
Abstract		iv
Table of Contents		vi
List of Tables		viii
List of Figures		ix
List of Abbreviations	x	
Introduction		
Fracture Overview		1
Endochondral and Intramembraneous Ossification		1
Fracture Healing		3
Bone Morphogenetic Proteins		6
Current Fracture Therapies		8
Methods		
Study Design		13
Surgery		14
Specimen Harvesting		17
Microcomputed Tomography		18
Three-Dimensional Rendering		20

Mechanical Testing	20
Statistical Analysis	22
Results	
MicroCT Testing	23
Mechanical Testing	29
Discussion	32
Conclusion	35
References	36
Curriculum Vitae	38

LIST OF TABLES

Table	Title	Page
1	MicroCT Data	25
2	Mechanical Testing Data	30

LIST OF FIGURES

Figure	Title	Page
1	Effects of PTH and PTHrP on osteoblasts	12
2	Apparatus used to produce unilateral femur fractures	16
3	Example X-ray of a right femur mid-diaphysis fracture	17
4	Graphical analysis of TV, BV, BV%, BMD, and TMD	26
5	Graphical analysis of Tb.N, Tb.Th, and Tb.Sp	27
6	Three-dimensional rendering of a sample in the 35 Day Delay group	28
7	Three-dimensional rendering of a sample in the 35 Day Continuous group	28
8	Three-dimensional rendering of a sample in the 35 Day Control	29
9	Graphical analysis of Max Torque, Stiffness, and Rigidity	31

LIST OF ABBREVIATIONS

BMD	Bone Mineral Density
BMP	Bone Morphogenetic Proteins
BV	Bone Volume
BV%	Bone Volume Percentage
Tb.N.	Trabecular Number
Tb.Sp.	Trabecular Spacing
Tb.Th.	Trabecular Thickness
TMD	Total Mineral Density
TV	Total Volume

INTRODUCTION

Fracture Overview

Fractures are among the most common large organ traumatic injuries. Fracture incidence is also increasing due to osteoporosis related fractures in the growing elderly population in the U.S. Fracture are such a common injury that a therapy developed to decrease healing time and increase bone strength after injury would have wide spread benefits in a large and growing population. Osteoporosis is the most common bone disease in the U.S. with an estimated 10 million Americans over the age of 50 inflicted with the disease and another 34 million at risk each year. An estimated half of all women over the age of 50 and one quarter of all men will experience a fracture due to osteoporosis. In 2002, the cost of care for osteoporotic fractures was estimated to be between \$12.2 to \$17.9 billion each year (USDHHS Office of the Surgeon General, 2004). The cost of care and incidences of osteoporotic related fractures are increasing each year as the growing population continues to age. It is estimated that by 2025 osteoporosis will be responsible for almost three million fractures and incur \$25.3 billion of costs each year (National Osteoporosis Foundation, 2013)

Endochondral and Intramembranous Ossification

To better understand the mechanism in which a fracture is healed it is important to review the two processes by which embryonic bone is formed and

how bones grow along the growth plate. These two important processes are endochondral and intramembranous ossification. The two processes differ in the fact that endochondral ossification requires a cartilage intermediate that is then replaced with bone while intramembranous ossification involves the direct conversion of mesenchymal cells into bone (Gilbert, 2000)

Endochondral bone formation, also known as endochondral ossification, is the process by which the bones of the axial and appendicular skeleton and lower mandible are initially formed. This process is also responsible for the elongation growth of long bones. Unlike intramembranous ossification, existing cartilage must be present for endochondral ossification to occur. The initial cartilage is formed through the condensation of mesenchymal cells, when then differentiates into chondrocytes. The chondrocytes undergo proliferation, hypertrophy, and secrete a specialized extracellular matrix to increase the length and size of the cartilage model (Mackie et al., 2008). Ossification starts at the primary and secondary centers of ossification located in the center of the diaphysis (primary center) and at each epiphysis (secondary centers). At these sites the cartilage matrix becomes mineralized and blood vessels invade the cartilage model bringing in osteoprogenitor cells and osteoclasts. The chondrocyte in these mineralized areas will undergo programmed cell death leaving behind their initial scaffold of mineralized tissue. As this process takes place, blood vessels will grow into these areas of mineralization, bringing mesenchymal stem cells with them. These stem cells will then differentiate into osteoprogenitor cells that will

then undergo differentiation into osteoblasts on these scaffolds and begin to deposit bone matrix while in other areas the osteoclasts will also remove some of the areas of mineralized cartilage matrix (Mackie et al., 2008).

Intramembranous ossification is responsible for the formation of the flat bones of the skull. The process of intramembranous ossification begins with the proliferation and condensation of mesenchymal cells into compact nodules. From these nodules, the mesenchymal cells differentiate into osteoblasts as well as capillaries (Gilbert, 2000). The osteoblasts secrete an osteoid matrix capable of binding calcium salts allowing the osteoid to become calcified into bone. Through this process some of the osteoblasts secreting the osteoid matrix become trapped within their own secretions and then become osteocytes. From the site of ossification, bony spicules radiate out which then become surrounded by mesenchymal cells that eventually form the periosteum (Gilbert, 2000). The periosteum is the membrane that surrounds the bone. Cells lining the inner part of the periosteum become osteoblasts and continue to secrete osteoid matrix leading the many layers of bone formation (Gilbert, 2000)

Fracture Healing

Fractures are a break in a bone that results from a force introduced to the bone that exceeds the bones strength or ability to absorb the force. Bones can become more susceptible to fractures from conditions such as osteoporosis that weaken the strength and integrity of the bone. Following a fracture to the bone,

the bone heals in two distinct processes. These processes are primary fracture healing and secondary fracture healing. Primary fracture healing is the process first responsible for uniting the separated broken cortex back together (Einhorn, 1998).

For primary fracture healing to occur, the cortices of both sides of the bone must join to reestablish mechanical continuity. Osteoclasts on one side of the fracture undergo a tunneling resorptive response that result in the formation of new Haversian systems, which provide routes for blood vessels to penetrate the site of injury (Einhorn, 1998). These blood vessels bring the necessary osteoprogenitor cells crucial for the formation and healing of the bone. This process of primary fracture healing can only occur if the fragments of the fracture are restored anatomically and if the fracture site is stabilized by rigid internal fixation (Einhorn, 1998).

During secondary fracture healing, both uncommitted osteoprogenitor cells and osteoblasts contribute to the fracture healing in a process paralleling both embryonic intramembranous ossification and endochondral bone formation. Secondary fracture healing is responsible for initially forming a callus to stabilize the fracture fragments. The periosteum and external soft tissues both play crucial roles in the process. Secondary fracture healing seems to be dependent on mechanical factors and is inhibited by rigid immobilization (Einhorn, 1998). During secondary fracture healing intramembranous ossification is seen on the proximal and distal sides away from the fracture site while endochondral

ossification is seen adjacent to the fracture site. The intramembranous ossification located further from the fracture site results in a “hard callus” which is the result of direct bone formation. The endochondral ossification forms a “soft callus” as a result of the early formation of cartilage which is later replaced by bone (Einhorn, 1998). The external soft tissue response also helps stabilize the bone fragments through endochondral ossification. This whole process is crucial for the rapid closure of the gaps produced by the fracture (Einhorn, 1998).

Fracture healing proceeds through 5 stages; hematoma formation and inflammation, angiogenesis and cartilage formation, cartilage calcification, cartilage removal and bone formation, and longer term bone remodeling (Einhorn, 1998). The formation of the hematoma and inflammation has been implicated in serving as source of signaling molecules which are important to initiate the cascade of steps in bone healing and formation. During the first 7 to 10 days woven bone appears opposed to the cortex near the fracture site resulting from intramembranous ossification. Adjacent to the fracture site, cartilage appears as result of the beginnings of endochondral ossification from the periosteum and external soft tissues (Einhorn, 1998). Starting after 10 days, the callus can be differentiated into the “hard” and “soft” callus. The callus tissue is formed primarily of cartilage, that then undergoes hypertrophic progression to a mineralized stage, that then undergoes vascular invasion and resorption and replacement by bone. At the “hard” callus section intramembranous ossification is occurring further from the fracture site and endochondral ossification is

occurring at the “soft” callus section. As the callus becomes fully mineralized more bone is created and the callus begins to undergo remodeling by osteoclasts. The bone is reshaped to its original structure with defined cortices and a new medullary space through a prolonged period of coupled remodeling (Gerstenfeld et al., 2003). Coupled remodeling is the result of the relationship between osteoblasts and osteoclasts. It depends on the anabolic rates of primary and secondary bone formation, as well as calcified cartilage resorption and primary bone remodeling (Gerstenfeld et al., 2005).

Bone Morphogenetic Proteins

Bone morphogenetic proteins (BMPs) are a group of growth factors that belong to the transforming growth factor- β (TGF- β) family. They were originally discovered as factors that could induce bone and cartilage formation when implanted at ectopic sites (Miyazono et al., 2009). BMPs have also been implicated in a number of biological activities in many different tissues and cell types. Dysfunctions in BMP pathways lead to many clinical disorders including vascular and skeletal diseases as well as cancer (Miyazono et al., 2009).

While there are many BMPs, for this study the focus will be on BMP-2 and BMP-4. BMP-2 and BMP-4 are closely related and share 83% of their amino acid sequence (Kawabata et al., 1998). BMP-2 and BMP-4 have been shown to be the stronger initiators of alkaline phosphatase activity and mesenchymal progenitor differentiation into osteoblasts (Miyazono et al., 2009). Both BMPs

have a wide range of biological activities in vivo as well as during embryonic development. Knockout of BMP-2, BMP-4, and bone morphogenetic protein receptor Type 1A (BMPR-1A) in a mouse model leads to embryonic death before bone development (Kamiya et al., 2008). Deficiency of BMP-2 in a mouse model has also shown that BMP-2 is necessary for the initiation of fracture healing. Mice lacking BMP-2 in their bones are unable to resolve spontaneous fractures and do not experience the earliest steps in fracture healing despite other osteogenic stimuli still being present (Tsuji et al., 2006).

Members of the TGF- β family bind two types of serine-threonine kinase receptors, type I and type II (Miyazono et al., 2009). BMPs can bind to both types independently, however when both types are present binding affinity increases drastically (Kawabata, 1998). Once a BMP has bound to a heterotypic receptor complex, the type II receptor will phosphorylate the type I receptor, which will in turn phosphorylate its intercellular second signal SMAD. The activated SMAD will then form a complex with another SMAD (Miyazono et al., 1998). Once the SMAD complex has been bound, the complex translocates to the nucleus where it carries out its biological effects by regulating the transcription of target genes by interacting with different transcription factors, activators, and repressors (Miyazono et al., 1998).

Although much of the signaling involved in osteogenesis is becoming better understood, much is still not clear. The mechanism by which BMP signaling in osteoblasts contributes to skeletogenesis is not fully understood

(Kamiya et al., 1998). Bone mass is determined by the relationship between bone formation and resorption. BMPs have been shown to play a role in both processes. However, the extent and to what degree BMPs have in each process is not clear. Loss of BMP signaling decreased bone volume in young mice, but increased bone mass in old mice (Kamiya et al., 1998). BMPR-1A deficient osteoblasts showed decreased osteoclastogenesis in mice (Kamiya et al., 1998). This implicates that by blocking that pathway, osteoclastogenesis was decreased which leads to fewer osteoclasts and decreased bone resorption.

Current Fracture Therapies

Currently there are a number of drug therapies approved for the treatment of osteoporosis. Bone remodeling is balanced by bone formation by osteoblasts and bone resorption by osteoclasts. These therapeutic agents follow 2 modes of action. They can act as an anti-resorptive agent or an anabolic agent. The anti-resorptive agents act by reducing osteoclastic activity. Bone resorption rates are decreased by reducing the catabolic effects of osteoclasts in osteoporosis patients. There is concern that prolonged inhibition of osteoclast activity and their role in repairing microdamage and other normal processes would be impeded and lead to eventual bone weakening (Pearsall et al., 2008). Anabolic agents act by increasing osteoblast-mediated bone formation and provide an attractive alternate therapy.

Bisphosphonates were the first anti-catabolic therapy that were approved and are the most widely and regularly used therapies for osteoporosis. Bisphosphonates act by inhibiting osteoclasts function, thereby inhibiting bone resorption which leads to an increase in bone mass due to refilling of the remodeling space and an increase in mineralized tissue density. Bisphosphonates bind to bone mineral with high affinity which allows for a high degree of organ specificity (Khosla et al., 2012). After binding to the bone, the bisphosphonates are taken up by osteoclasts. Once inside the osteoclasts, the bisphosphonate blocks specific metabolic pathways that are needed for the osteoclasts to function which disrupts cellular function and promotes apoptosis (Khosla et al., 2012). In women, bone remodeling rates increase by double within 12 months of menopause, triple by the age of 60, and remain elevated in untreated osteoporosis patients (Khosla et al., 2012). Administration of bisphosphonates reduces the rate of bone remodeling associated with microdamage repair. Bisphosphonates are able to induce their therapeutic effect by inhibiting osteoclasts and decrease fracture incidences in osteoporosis patients. Experimental studies have shown that bisphosphonate administration results in larger and stronger calluses, delayed remodeling, and no evidence of delayed healing (Larsson et al., 2012). Bisphosphonates have been associated with some negative side effects but the rare rate of their occurrence does not outweigh the therapeutic effects they provide. Possible negative side effects that

have been implicated with bisphosphonates include osteonecrosis of the jaw, atypical femur fractures, and atrial fibrillation (Khosla et al., 2012).

An alternate therapy that closely mirrors the mechanism by which bisphosphonates work to help osteoporosis patients is the use of bacillus fermented antlers. Antlers have been used throughout history for its claimed medicinal and therapeutic properties. Use of bacillus fermented antlers has shown to inhibit osteoclast differentiation and osteoclast regulated bone resorption (Choi et al., 2013). Addition of the fermentation to the antler has shown to increase its osteogenic properties (Choi et al., 2013).

Receptor activator of NF kappa B ligand (RANKL) inhibitors have recently been developed as a possible treatment for osteoporosis. RANKL inhibitors work by inhibiting osteoclasts precursor cells into osteoclasts (Larsson et al., 2012). When compared with the bisphosphonate alendronate, RANKL inhibitor denosumab produced very similar results on fracture healing. Both drug groups showed increased callus volume, callus cross-sectional area, and increased mineral density when compared with the controls (Gerstenfeld et al., 2008). Both groups also showed increased callus strength under mechanical testing, but it is important to note that most of the RANKL denosumab group fractures occurred outside the callus tissue indicating increased callus strength over the bisphosphonate alendronate group (Gerstenfeld et al, 2008).

Parathyroid hormone (PTH) has also been extensively researched a possible osteoporosis therapy. Anabolic drugs exert their effects by positively

enhancing bone formation, instead of having a negative effect on osteoclast activity like all of the other treatments discussed so far. The positive effects of anabolic therapy are an attractive possibility for fracture healing therapies. The effects of PTH vary depending on the administration regimen. When administered continuously, bone resorption is increased due to an increase in osteoclastic activity. When administered intermittently, bone formation is increased due to increased osteoblast activity (Larsson et al, 2012). Studies have shown that PTH administration for fracture healing resulted in larger and mechanically stronger calluses in less time (Larsson et al., 2012). A diagram of PTH and PTH-related protein effects on osteoblasts can be seen in figure 1.

The drug used in this study, RAP-661, is a soluble receptor fusion protein consisting of the extracellular domain of the activin receptor-like kinase-3 (ALK-3) Type I receptor, also known as BMPR-1A, fused to a murine IgG2a antibody Fc region. RAP-661 acts as an antagonist by binding BMP-2 and BMP-4 with high affinity and blocking their signaling through their BMPRs.

Current Goals

The aim of the study was to investigate the therapeutic efficacy of RAP-661 in improving fracture healing. The growing incidences of fractures due to osteoporosis as well as the already high incidence rate of fractures in healthy individuals in the country could benefit immensely from a therapy that could increase bone strength post-fracture and decrease fracture healing time. In

addition to the health benefits, the cost of care for osteoporosis related fractures could be decreased incrementally. The main focus of this study was to assess the effect of the RAP-661 protein on both the regain of mineralized tissue and mechanical competency after fracture. The effect of the RAP-661 protein on fracture healing was assessed through microCT analysis and mechanical testing.

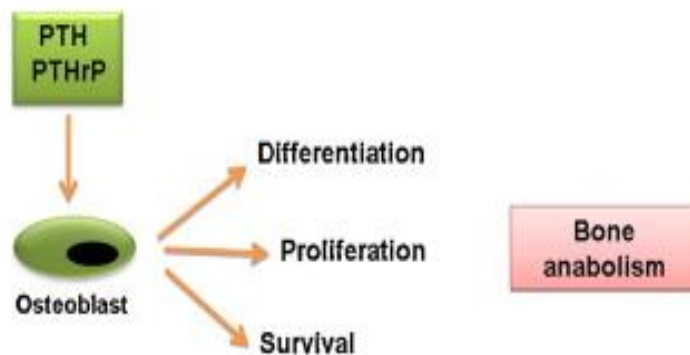


Figure 1. Effects of PTH and PTHrP on osteoblasts and bone anabolism (Esbrit et al., 2013).

MATERIALS AND METHODS

Study Design

All aspects of these animal studies was carried out under a protocol that has been approved by the Boston Institutional Animal Care and Use Committee and were conducted in conformity with all federal and USDA guidelines. Male mice at sexual maturity between 10-12 weeks of age were used for these studies. C57/B6 mice were ordered from Jackson Laboratories, Bar Harbor, ME and were shipped directly to Boston University Laboratory Animal Science Center (LASC), Boston, MA. All of the mice were housed at the LASC for the duration of the study as well as an additional 3 days when first shipped for acclimation to the facilities.

Three study groups used for the study were: The vehicle treated control group (10 mM Tris-Buffered Saline), the continuous group that was administered RAP-661 in 10 mM TBS continuously from time of fracture, and the delay group that was administered RAP-661 in 10 mM TBS continuously starting 14 days post fracture. The three groups were terminally harvested at 35 days. For the microCT analysis the 35 Day Delay group consisted of 12 mice, the 35 Day Continuous group consisted of 10 mice, and the 35 Day Control group consisted of 12 mice. For mechanical testing the 35 Day Delay group consisted of 10 mice, the 35 Day Continuous group consisted of 8 mice, and the 35 Day Control consisted of 10 mice.

Both drug and vehicle were administered via intraperitoneal injection twice per week. RAP-661 was administered at 10mg/kg for each injection. Prior to administration, all drugs were warmed to room temperature and administered via a 25-gauge needle.

Surgery

Starting at Day 0 (day of surgery), all animals were subjected to a unilateral fracture in the right femur. All fractures were produced with a modified device as described by (Marturano et al., 2008) of the original apparatus described by Bonnerans and Einhorn (1984). A picture of the device can be seen in figure 1. Prior to surgery each animal was anesthetized with isoflurane. After anesthization, the right rear leg was shaved and disinfected with povidone iodine skin disinfectant. A median longitudinal skin incision was introduced over the distal femur. A hole was created by inserting the stylette of a 25 gauge spinal needle though the trochlea of the femur. The pin was inserted in a retrograde manner and anchored in the major trochanter with gentle rotation. The stylette was cut at the condylar surface and buried by pushing it through the cartilage into the underlying subcondylar bone. The incision was closed with one internal suture. Unilateral fractures were produced in the mid-shaft of the right femur using the scaled down version of the apparatus described by Bonnarens and Einhorn, 1984. Confirmation of the fracture location and quality was confirmed by X-ray analysis directly following the production of the unilateral fracture using

a GenDex Dental X-ray machine. All X-rays were developed right after pin insertion and fracture by a portable x-ray developer. All fractures that were determined to be unsuitable for reasons such as non-medial fractures or were inconsistent with standardized criteria were not used for the study. An example of X-ray image of a suitable mid-diaphysis fracture can be seen in figure 2.

After X-ray analysis, each animal was subjected to an ear-cut identification. This was accomplished by punching a hole in either the right ear, left ear, both ears, or no ears. 0.5 mg/kg of Buprenex® (buprenorphine) was delivered subcutaneously for post-operative pain management. Additionally, the anti-biotic Baytril® was administered at a dosage of 2.5 mg/kg and delivered subcutaneous at the time of surgery. Each animal then received 0.5 mg/kg of buprenorphine analgesia every 12 hours for 24 hours post fracture as well as one dose at 48 hours.

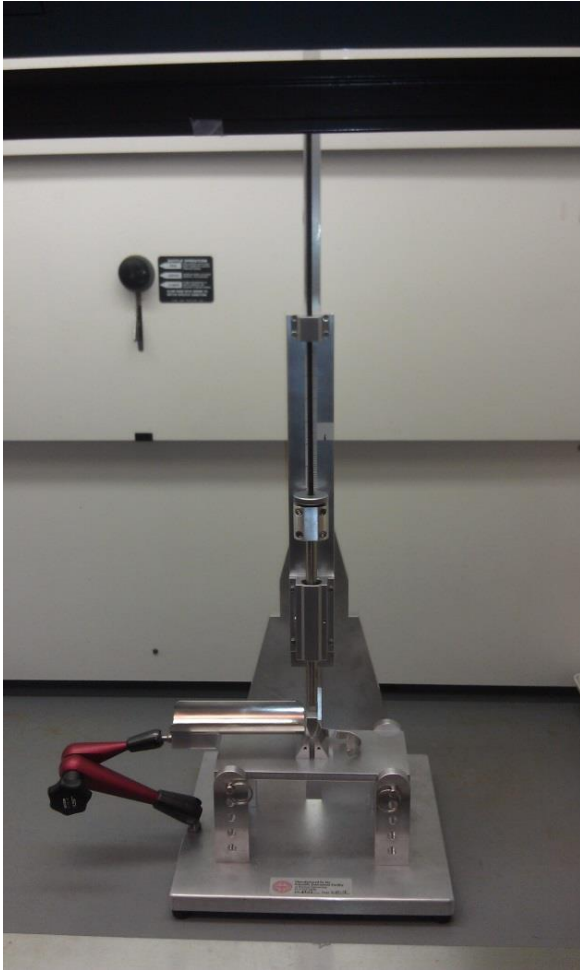


Figure 2. Device used to produce unilateral fractures in the mouse femurs.

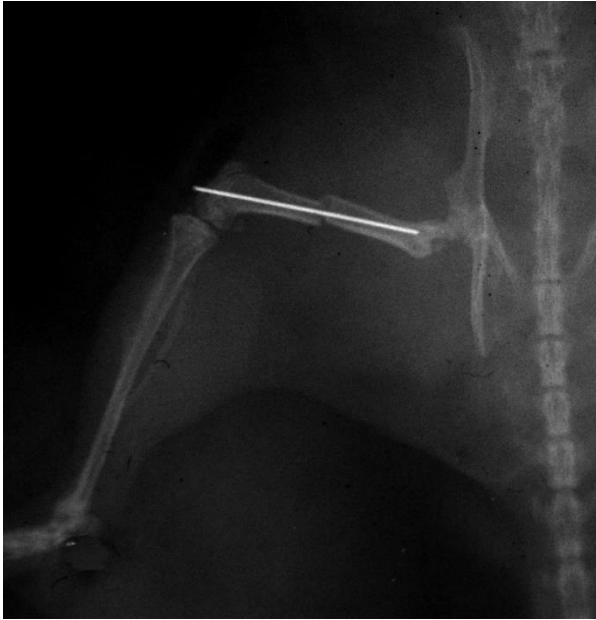


Figure 3. Example of a right femur mid-diaphysis fracture with 25-gauge spinal needle stylette present in the medullary canal (Sacks, 2007).

Specimen Harvesting

At time of harvest (35days), all mice were euthanized by CO₂ asphyxiation followed by secondary euthanasia by cervical dislocation. After euthanasia, all fractures were evaluated radiologically by use of a Faxitron X-ray system. After X-ray, both the fractured femora as well as the contralateral femora were excised by disarticulation of the limbs. After all surrounding soft tissue and skin was removed; the femur was wrapped in sterile isotonic saline soaked gauze, placed in a labeled test tube, and dropped into liquid nitrogen. All samples were kept in the liquid nitrogen until all samples had been finished being harvested. Once harvesting was completed, all samples were placed in a marked box which was then placed in a -20° C freezer.

Microcomputed Tomography

To determine mineralized tissue content and structure, calluses from the 35 day time points were scanned at an isotropic voxel size of 12 μm (70 kVp, 114mA, 200ms integration time; μCT 40, Scanco Medical, Bruttisellen, Switzerland). All bones intended for scanning were transported from a -20°C freezer in the Boston University Orthopaedic Research Laboratory to a -20°C freezer in the Boston University Orthopaedic and Developmental Biomechanics Laboratory.

All bones were thawed at room temperature and then removed from the wrapping gauze. Depending on the size of the bone and its callus, a piece of packing Styrofoam was cut to insert along with the bone to ensure the bone did not move during scanning. The bone and the Styrofoam insert were placed vertically inside the microCT tube. Multiple bones up to a maximum of 3 were able to be placed inside the microCT tube at a time. Each bone was placed with its own Styrofoam insert and were only stacked vertically on top of each other. Once all of the bones were placed in the microCT tube, the tube was filled with PBS. All air bubbles were removed and the top was covered by a piece of Parafilm (Alcan Packaging, Neenah, WI). The area of interest to be scanned was manually selected. The area was selected to only include the callus and a small area directly below and above callus to ensure the whole callus was included. Scans were performed at a medium resolution (12 μm voxel size) at 70 kVp, 114 μA , and 200 ms integration time.

Following scanning, all of the tomograms were contoured manually to define the boundary of the callus and to exclude all cortical bone and the medullary canal. To define the inclusion portion of the callus, a rough counter-clockwise trace of the outline of the callus was performed and the computer program selected the exact outline. To establish the exclusion portion of the callus, a clockwise trace of the cortical bone and medullary canal was performed manually to exact boundaries without aid of the computer program. Cortical bone was distinguished by its much denser white color towards the center of the callus and was excluded. Pieces of cortical bone that did not correspond to the medullary canal were also excluded by additional manual contours for the slices that they appeared. The area between the inclusion boundary and exclusion boundary was used to perform all computations by the program for all desired data. A fixed global threshold corresponding to 45% of the attenuation of the mature cortical bone was applied (Morgan *et al.*, 2009). Once the volume of interest was defined, the tomograms for each bone were evaluated to determine total volume (TV), mineralized volume (BV), mineralized volume fraction (BV/TV), tissue mineral density (TMD), bone mineralized content (BMC, defined as $BV * TMD$), trabecular number (Tb.N), trabecular spacing (Tb.S), and trabecular thickness (Tb.Th).

Three-Dimensional Rendering

Following scanning, all of the tomograms were contoured manually to define the boundary of the callus and to exclude all cortical bone and the medullary canal. Once contoured, the SCANCO computer #D viewer program was able to construct three dimensional images of the fracture callus.

Mechanical Testing

All bones intended for mechanical testing were transported from a -20° C freezer in the Boston University Orthopaedic Research Laboratory to a -20° C freezer in the Boston University Orthopaedic and Developmental Biomechanics laboratory. For these studies this set of bones was sequentially assayed by microCT and mechanical testing. These bones were first scanned individually and were thawed during the scanning process. Bones intended for mechanical testing were placed in the microCT tubes with a solution of 40% ethanol and 60% phosphate buffered saline (PBS). Directly following scanning, each bone was wrapped in gauze soaked in the alcohol-saline solution to ensure the bone remained hydrated. While the bone was wrapped, a clamp was attached to a clamp stand and a set of forceps were placed in the clamp. The bone was then placed gently into the forceps ensuring not to clamp any of the callus. Two aluminum end cubes (1 cm³) were placed on two over turned paper cups. Next, another paper cup was cut to make a shallow cup. Bosworth Fastray powder and Bosworth Fastray solvent were then mixed in the cup to create liquid

polymethylmethacrylate (PMMA). The consistency of the liquid PMMA was made at a low viscosity to ensure full encapsulation of the end of the bone placed in the PMMA. Using a pipette, the liquid PMMA was transferred from the cup to the cap intended for the bone to first be placed and filled to the top. PMMA was transferred into the second cap but was only filled half way. The bone was then lowered into the primary cap by loosening the clamp from the clamp stand and slowly moving the clamp flush against the stand until the tip of the bone was submerged in the PMMA and then retightening the clamp. The bone was only lowered into the PMMA close to the callus but never made contact with the callus. After a few minutes, the top of the PMMA was hardened enough to place a small wrap of alcohol-saline soaked gauze around the bone. The PMMA was hard enough to ensure no PMMA would be soaked up by the gauze. The system was then allowed to sit for approximately 30 minutes for the PMMA to completely harden. After the 30 minutes, both the cap with the bone and the half-filled cap were removed from the over-turned Dixie Cups. All PMMA that accumulated from leaking at the end of the caps were removed to ensure the caps could lay flat on all 5 sides. The caps were then placed flush in a L Beam and held in place by rubber bands. Approximately 1 cm was left between the caps the whole system was clamped onto a clamp stand. A second batch of liquid PMMA was made by the same procedure. Using a pipette, the liquid PMMA was transferred to the half-filled cap and filled all the way. Once completely filled, the caps were pushed towards each other slowly until the uncovered end of the bone was

submerged. After approximately 5 minutes, another saline-alcohol gauze piece was wrapped around the bone. The system was allowed to sit for another 30 minutes to completely dry.

Immediately after the specimen was potted, the gauge length was measured by calipers. The system was then placed into the clamps of the Instron 55MT Micro Torsion Testing System (Instron, Norwood, MA) ensuring not to introduce any stress on the callus. Once placed into the machine the protocol was run to apply an angular rotation of 0.5 degrees/sec. The Instron 55MT Micro Torsion Testing System plotted and collected the data which was then saved and exported for further evaluation. The data of interest collected was maximal torque to failure, stiffness, and rigidity.

Statistical Analysis

The effects of treatment on each group were determined using analysis of variance (ANOVA) with Tukey *post hoc* tests. The significance level of 0.05 was used for all analyses.

RESULTS

MicroCT Testing

A total of 34 bones were analyzed via microCT. Of the 34 bones 12 were in the 35 day delayed drug treatment group, 10 were in the 35 day continuous drug treatment group, and 12 were in the 35 day control non-treated group. A summary of the microCT data is presented in Table 1 and the comparisons between the three groups can be seen for each data category in figures 1-2.

From the figures, some noticeable differences can be discerned. For every category except for Total Volume (TV), the two treated drug groups are higher than the control. For TV, the 35 Day Continuous group is the smallest, but when Bone Volume / Total Volume (BV%) is taken into account, we can see that the 35 Day Continuous group has the highest BV%. Through analysis with one way analyses of variances (ANOVA), significant differences were found in BV%, total mineral density (TMD), bone mineral density (BMD), trabecular spacing (Tb.Sp), and trabecular Number (Tb.N) at an alpha level = .05. There were no significant differences found in TV or bone volume (BV). The 35 Day Delay treatment has the highest BV, followed by the 35 Day Continuous treatment, while the 35 Day Control showed the lowest values for these parameters. For BV% we can see that 35 Day Continuous was the highest and was significantly different from both 35 Day Delay and 35 Day Control. TV was the lowest in the 35 Day Continuous treatment and could be a reason for the higher BV%. For

TMD, the 35 Day Continuous treatment was the highest and was significantly different from both the 35 Day Delay and 35 Day Control treatments. For Tb.N, the 35 Day Continuous treatment was the highest, followed by the 35 Day Delay treatment and then the 35 Day Control. All treatments were significantly different from each other for Tb.N. For Tb.Th, the 35 Day Continuous Treatment was the highest, followed the 35 Day Delay treatment and then the 35 Day Control. The 35 Day Continuous treatment was significantly different from the 35 Day Control group. For Tb.Sp, the 35 Day Control group was the highest, followed by the 35 Day Delay treatment and then the 35 Day Continuous treatment. The 35 Day Control group was significantly different from both other groups.

A three-dimensional rendering was created for a specimen in each of the groups. These renderings can be seen in figures 3-5.

Table 1. MicroCT Analysis

	35 Day		
	35 Day Delay	Continuous	35 Day Control
TV (mm³)	23.28 ± 12.08	16.39 ± 5.94	21.66 ± 8.12
BV (mm³)	5.88 ± 2.52	5.77 ± 1.69	4.96 ± 1.74
BV%	27.90 ± 9.51 ⁽²⁾	36.10 ± 4.64 ^(1,3)	23.60 ± 4.37 ⁽²⁾
TMD (mg HA/ccm)	449.42 ± 100.97 ⁽²⁾	544.92 ± 47.74 ^(1,3)	389.36 ± 49.67 ⁽²⁾
BMD (mg HA/ccm)	1191.86 ± 23.72 ⁽²⁾	1215.32 ± 14.37 ^(1,3)	1191.79 ± 26.72 ⁽²⁾
Tb.N (1/mm)	4.85 ± 0.72 ^(2,3)	5.62 ± 0.52 ^(1,3)	3.83 ± 0.54 ^(1,2)
Tb.Th (mm)	0.11 ± 0.016	0.12 ± 0.016 ⁽³⁾	0.094 ± 0.012 ⁽²⁾
Tb.Sp (mm)	0.22 ± 0.035 ⁽³⁾	0.18 ± 0.021 ⁽³⁾	0.27 ± 0.037 ^(1,2)

Data shown are mean values ± SD. Significant differences between 35 Day Delay, 35 Day Continuous, or 35 Day Control are shown by 1, 2, or 3, respectively.

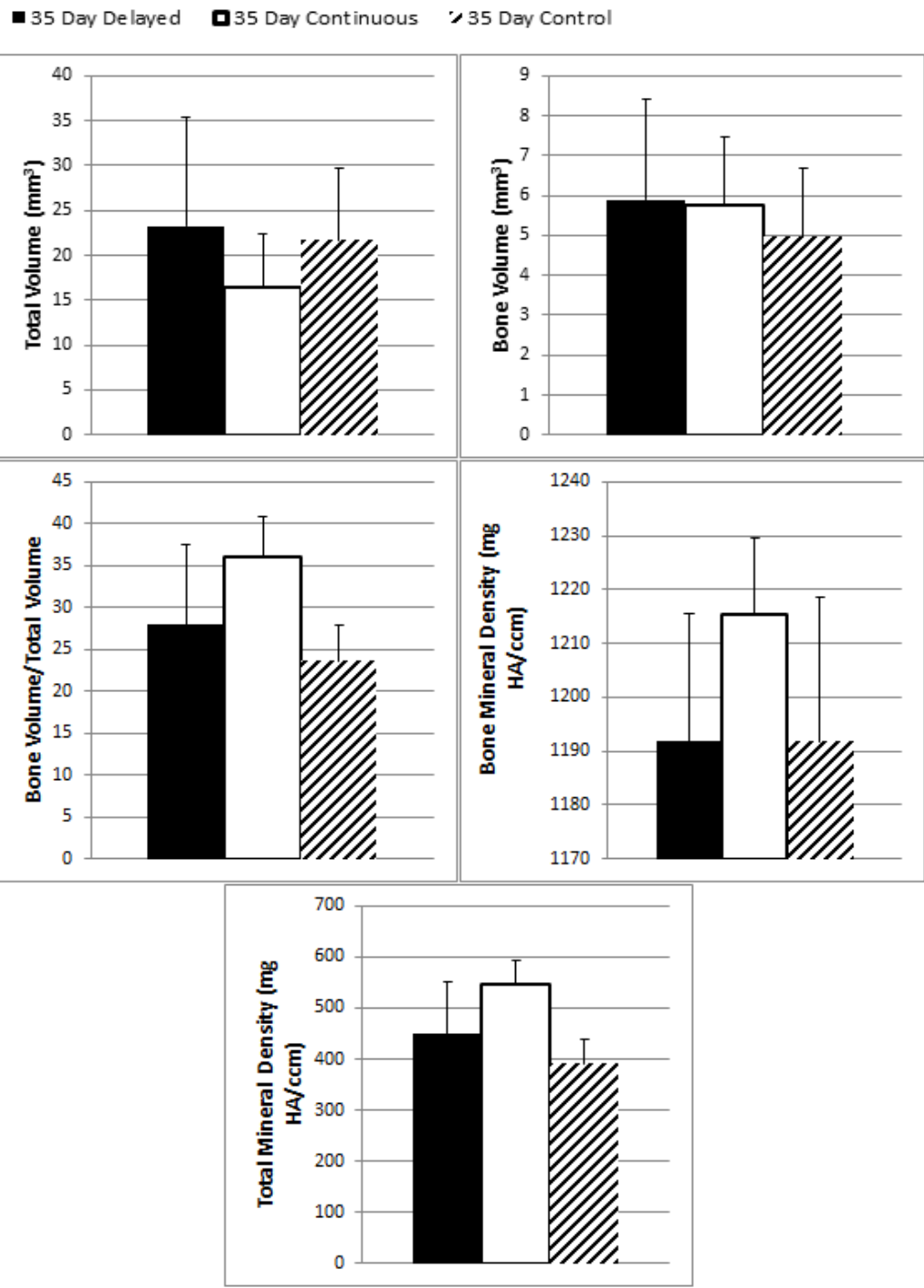


Fig. 4. Graphical analysis of TV, BV, BV%, BMD, and TMD.

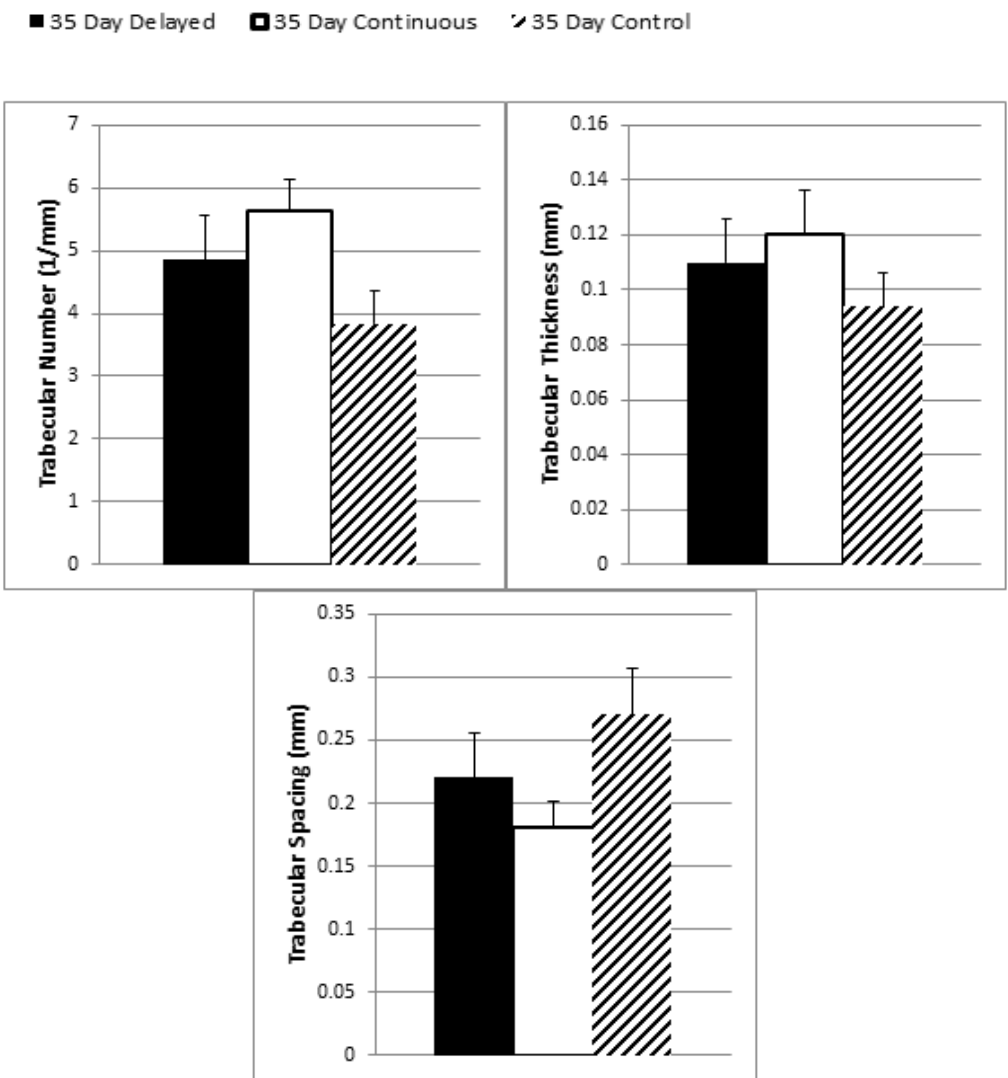
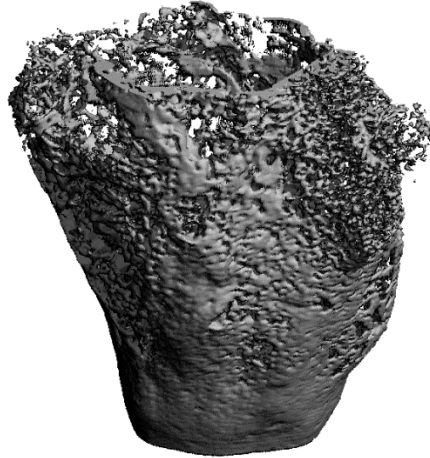


Fig. 5. Graphical analysis of Tb.N, Tb.Th, and Tb.Sp.

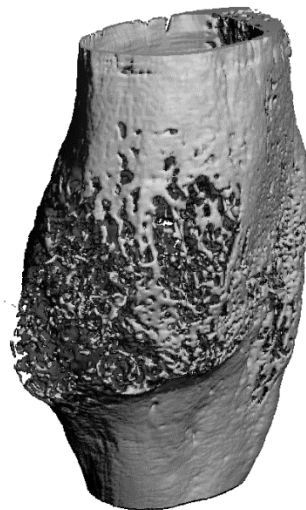
Alex_Accel_171



1.0 mm

Figure 6. Three-dimensional rendering of a sample in the 35 Day Delay group.

Alex_Accel_187



1.0 mm

Figure 7. Three-dimensional rendering of a sample in the 35 Day Continuous group.

Alex_FTH-B6_38

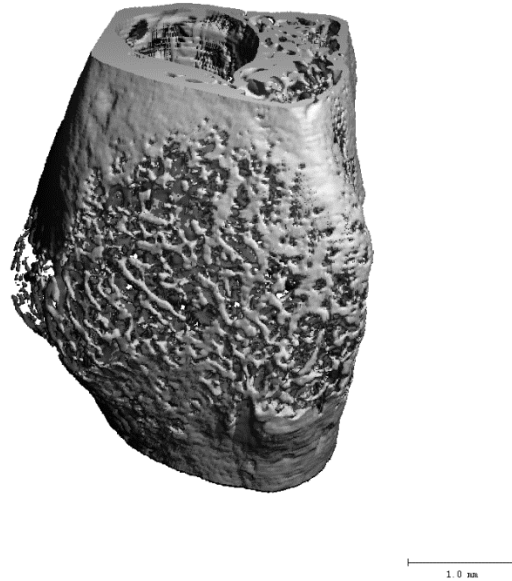


Figure 8. Three-dimensional rendering of a sample in the 35 Day Control.

Mechanical Testing

A total of 28 bones were analyzed via mechanical testing. Of the 28 bones 10 were in the 35 day delayed drug treatment group, 8 were in the 35 day continuous drug treatment group, and 10 were in the 35 day control non-treated group. Two bones in the 35 day delayed drug treatment group, two bones in 35 day continuous treatment group were broken, and two bones in the 35 day control group were broken and could not be used for mechanical testing from the original group of bones that were scanned via microCT. A summary of the mechanical testing data is presented in Table 2 and the comparisons between the three groups can be seen for each data category in figure 3.

The 35 Day Control had the highest max torque and was significantly different than both of the treated groups. The 35 Day control also had the highest stiffness and rigidity, followed by the 35 Day Delay group and then the 35 Day Continuous Group. Differences in stiffness and rigidity were not significant.

Table 2. Mechanical Testing Data

	35 Day		
	35 Day Delay	Continuous	35 Day Control
Max Torque (N•mm)	0.023 ± 0.007 ⁽³⁾	0.024 ± 0.006 ⁽³⁾	0.039 ± 0.007 ^(1,2)
Stiffness (Nm/rad)	0.478 ± 0.170	0.381 ± 0.091	.494 ± 0.135
Rigidity (N/rad)	0.109 ± 0.056	0.065 ± 0.018	.114 ± 0.056

Data shown are mean values ± SD. Significant differences between 35 Day Delay, 35 Day Continuous, or 35 Day Control are shown by 1, 2, or 3, respectively.

■ 35 Day Delayed ■ 35 Day Continuous ▨ 35 Day Control

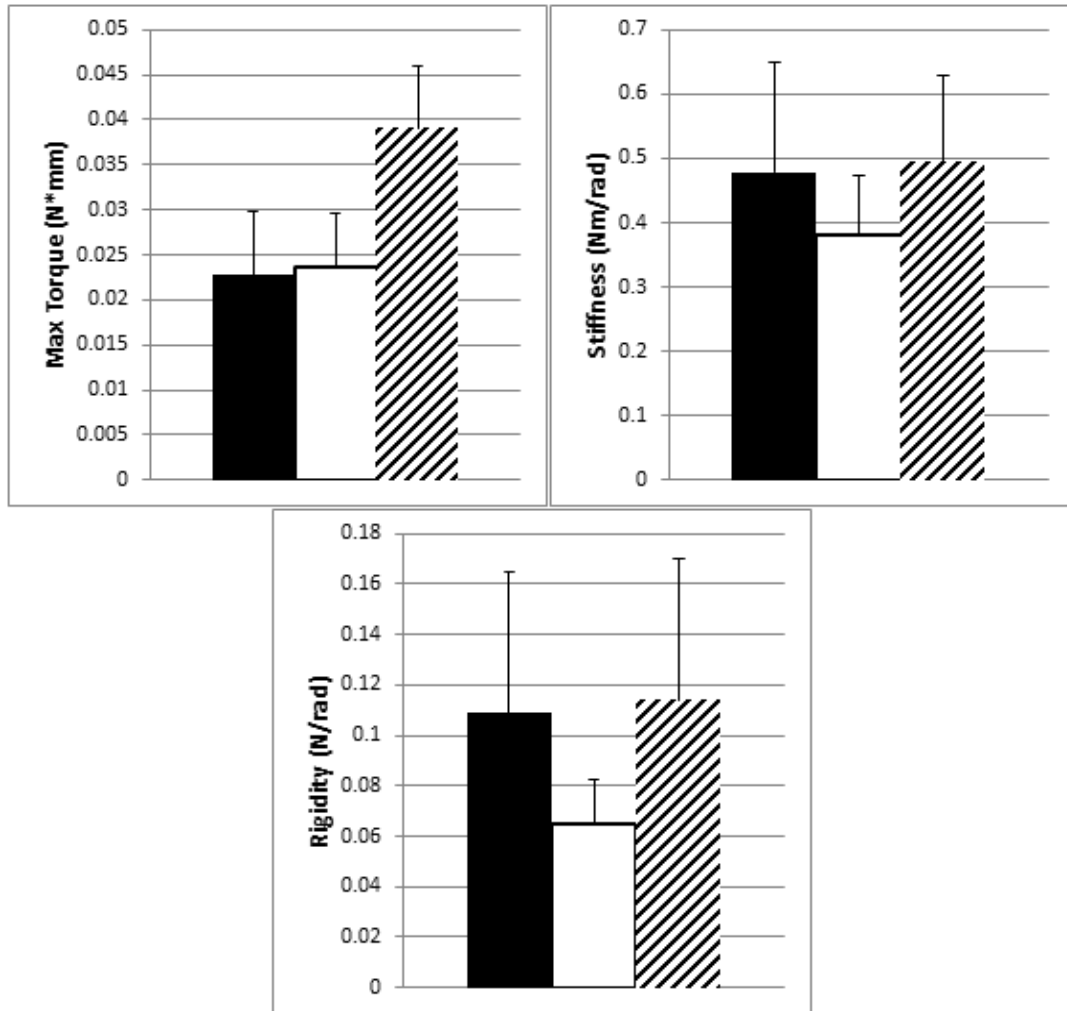


Fig. 9. Graphical analysis of Max Torque, Stiffness, and Rigidity.

Discussion

The primary goal of fracture healing therapies is to increase fracture callus strength and decrease fracture healing time. Development of such therapies would address a major clinical problem that the US is encountering with increased frequency due to the increasing number of osteoporosis related fractures. The purpose of this study was to evaluate the efficacy of RAP-661, an antagonist that binds BMP-2 and BMP-4 and blocks their pathways, as a possible drug therapy for fracture healing. Optimal fracture healing occurs when the structural integrity to the injured bone has been reestablished so that it may again experience stresses without incurring further damage. The anti-resorptive/anti-catabolic therapies that have been on the market for years for osteoporosis have shown great therapeutic effects however; very little investigation has been done on bone healing (Larsson, 2012). In this regard, studies have been examining a number of anabolic therapies including PTH and anti-sost therapies (Ke et al., 2012, Axelrad et al, 2007).

Our results showed that continuous drug treatment lead to a significantly smaller overall callus volume, while delaying the treatment lead to overall callus sizes comparable to the controls. Interestingly, the overall bone volume in both drug treatment groups was greater. The greater overall BV for both treatment groups lead to the continuous treatment group having the highest mineral density and highest BV%. The fact that the BV% of the 35 Day Continuous was

significantly different than the other two groups could be explained by two reasons. The continuous treatment had the smallest TV, so in comparison to BV the ratio would lead to a higher BV%. The continuous treatment could also have led to a greater amount of mineralized tissue. The smaller TV in the 35 Day Continuous group compared to the other groups can also be seen in the three dimensional renderings in figures 3-5.

The increased BV and BV% in both treated groups compared to the control group were consistent with our original expectation based on results seen when osteoporotic animals had been treated with the drug. These results further lead us to initially speculate that the strength of the callus would also be increased, however this is not what was observed. From the mechanical test data, we observed that the control experienced almost twice the max torque than both of the treated groups. This observation illustrates a large discordance between the two sets of data, which has not been previously observed in other pharmacological studies, in which we had always observed a strong correlation between both BMD and BV% and mechanical strength (Morgan et al., 2009). This discordance indicates that even though there was increased BV and BV%, the increase in mineralized tissue did not correlate to a stronger callus.

Since the structural bridging of the external cortices over the callus is a major element in the regain in mechanical strength, a possible explanation for this phenomenon must be related with the structural elements of the callus. The structural failure of the callus could only be explained by a failure of bridging. A

failure of bridging could explain the lower max torques observed and still allow for increased BV and BV%. The increased BV could have just been in the surrounding callus but not contribute to the bridging of the fracture site. Other possible explanations could be decreased or lack of cortical bone or decreased cross-sectional callus area. While these are possible explanations, further evaluation must be done to determine the mechanism behind this observation.

While not significant, we observed a higher stiffness and rigidity in the 35 Day Delayed group compared to the 35 Day Continuous group. This could indicate that by delaying the treatment, the callus was able to establish an initial effort to structurally repair the callus.

When compared to other treatments, RAP-661 does not seem like a favorable choice as a therapy for fracture healing. These data also suggest that if the drug was being used as an anti-osteoporosis therapy, its discontinuation would have to be considered in the case of a fracture injury, since their fracture healing would be impaired.

Conclusion

The purpose of this study was to assess the effectiveness of the RAP-661 protein as a therapeutic agent for fracture healing. C57/B6 mice had transverse fractures produced in the right femora and were administered either RAP-661 continuously, RAP-661 delayed, or PBS (control) following the fracture. The animals were harvested at 7, 14, 21, or 35 days post fracture. The femora were analyzed by microCT and torsion testing. Results showed that at the 35 day time point the two drug groups showed increased BV% but decreased mechanical strength compared to the control. The 35 Day Delay group showed incrementally larger max torque, stiffness, and rigidity which could indicate by delaying administration of the RAP-661 an initial bridging of the callus could occur, increasing mechanical strength. The discordance between the increased mineralized tissue and decreased mechanical strength will require further research. Further research using histology will be very helpful in elucidating what could be leading to the weaker calluses, regardless of the increased mineralized tissue. In the future, long term studies will need to be conducted to further our understanding of the mechanism that RAP-661 is increasing callus size and mineralized tissue without increasing callus strength. In the current short-term study, RAP-661 does not look like viable osteoporosis or fracture healing therapy due to its negative effects on callus strength.

REFERENCES

- Axelrad, T., Kakar, S., & Einhorn, T. (2007). New technologies for the enhancement of skeletal repair. *Injury*.
- Choi, S.-W., Moon, S.-H., Yang, H. J., Kwon, D. Y., Son, Y.-J., Yu, R., ... Kim, S. H. (2013). Antiresorptive Activity of Bacillus-Fermented Antler Extracts: Inhibition of Osteoclast Differentiation. *Evidence-Based Complementary and Alternative Medicine*, 2013, 1–9. doi:10.1155/2013/748687
- Department of Health and Human Services. (2004). *Bone Health and Osteoporosis A Report of the Surgeon General*. Rockville, MD: Office of the Surgeon General.
- Esbrit, P., & Alcaraz, M. J. (2013). Current perspectives on parathyroid hormone (PTH) and PTH-related protein (PTHrP) as bone anabolic therapies. *Biochemical Pharmacology*. doi:10.1016/j.bcp.2013.03.002
- Gerstenfeld, L. C., Sacks, D. J., Pelis, M., Mason, Z. D., Graves, D. T., Barrero, M., ... Einhorn, T. A. (2009). Comparison of Effects of the Bisphosphonate Alendronate Versus the RANKL Inhibitor Denosumab on Murine Fracture Healing. *Journal of Bone and Mineral Research*, 24(2), 196–208. doi:10.1359/jbmr.081113
- Gerstenfeld, L., Cullinane, D., Barnes, G., Graves, D., & Einhorn, T. (2003). Fracture Healing as a Post-Natal Development Process: Molecular, Spatial, and Temporal Aspects of Its Regulation. *Journal of Cellular Biochemistry*, 873-884.
- Gerstenfeld, L. C., Wronski, T. J., Hollinger, J. O., & Einhorn, T. A. (2005). Application of Histomorphometric Methods to the Study of Bone Repair. *Journal of Bone and Mineral Research*, 20(10), 1715–1722. doi:10.1359/JBMR.050702
- Gilbert SF. Developmental Biology. 6th edition. Sunderland (MA): Sinauer Associates; 2000. Osteogenesis: The Development of Bones. Available from: <http://www.ncbi.nlm.nih.gov/books/NBK10056/>
- Kamiya, N., Ye, L., Kobayashi, T., Mochida, Y., Yamauchi, M., Kronenberg, H., . . . Mishina, Y. (2008). BMP Signaling negatively regulates bone mass through sclerostin by inhibiting the canonical Wnt pathway. *Development and Disease*, 3801-3811.
- Kawabata, M., Imamura, T., & Miyazono, K. (1998). Signal transduction by bone morphogenetic proteins. *Cytokine & Growth Factor Reviews*, 9(1), 49–61. doi:10.1016/S1359-6101(97)00036-1
- Ke, H., Richards, W., & Ominsky, M. (2012). Sclerostin and Dickkopf-1 as therapeutic targets in bone diseases. *Endocrine Reviews*, 747-783.
- Khosla, S., Bilezikian, J. P., Dempster, D. W., Lewiecki, E. M., Miller, P. D., Neer, R. M., ... Potts, J. T. (2012). Benefits and Risks of Bisphosphonate Therapy for Osteoporosis. *Journal of Clinical Endocrinology & Metabolism*, 97(7), 2272–2282. doi:10.1210/jc.2012-1027
- Larsson, S., & Fazzalari, N. L. (2012). Anti-osteoporosis therapy and fracture healing. *Archives of orthopaedic and trauma surgery*. doi:10.1007/s00402-012-1558-8

- Lissenberg-Thunnissen, S. N., De Gorter, D. J. J., Sier, C. F. M., & Schipper, I. B. (2011). Use and efficacy of bone morphogenetic proteins in fracture healing. *International Orthopaedics*, 35(9), 1271–1280. doi:10.1007/s00264-011-1301-z
- Mackie, E. J., Ahmed, Y. A., Tatarczuch, L., Chen, K.-S., & Mirams, M. (2008). Endochondral ossification: How cartilage is converted into bone in the developing skeleton. *The International Journal of Biochemistry & Cell Biology*, 40(1), 46–62. doi:10.1016/j.biocel.2007.06.009
- Marsell, R., & Einhorn, T. A. (2011). The biology of fracture healing. *Injury*, 42(6), 551–555. doi:10.1016/j.injury.2011.03.031
- Marturano, J. E., Cleveland, B. C., Byrne, M. A., O'Connell, S. L., Wixted, J. J., & Billiar, K. L. (2008). An improved murine femur fracture device for bone healing studies. *Journal of Biomechanics*, 41(6), 1222–1228. doi:10.1016/j.jbiomech.2008.01.029
- McClung, M., Harris, S. T., Miller, P. D., Bauer, D. C., Davison, K. S., Dian, L., ... Lewiecki, E. M. (2013). Bisphosphonate Therapy for Osteoporosis: Benefits, Risks, and Drug Holiday. *The American Journal of Medicine*, 126(1), 13–20. doi:10.1016/j.amjmed.2012.06.023
- Miyazono, K., Kamiya, Y., & Morikawa, M. (2009). Bone morphogenetic protein receptors and signal transduction. *The Journal of Biochemistry*, 35-51.
- Morgan, E., Mason, Z., Chien, K., Pfeiffer, A., Barnes, G., Einhorn, T., & Gerstenfeld, L. (2009). Micro-computed tomography assessment of fracture healing: relationships among callus structure, composition, and mechanical function. *Bone*, 335-344.
- National Osteoporosis Foundation. What is Osteoporosis?. Available at: <http://www.nof.org/articles/7>. Accessed on March 15, 2013.
- Pearsall, S., Canalis, E., Cornwall-Brady, M., Underwood, K., Haigis, B., Urcan, J., ... Bouxsein, M. (2008). A soluble activin TypeIIA receptor induces bone formation and improves skeletal integrity. *Proceedings of the National Academy of Sciences*, 105(19), 7081–7087.
- Sacks, D. (2007). *Effects of a bisphosphonate (alendronate) and a RANKL inhibitor (AMG 162/ Denosumab) on fracture healing in a mouse model* (Unpublished master's thesis). Boston University, Boston, MA.
- Tsuji, K., Bandyopadhyay, A., Harfe, B. D., Cox, K., Kakar, S., Gerstenfeld, L., ... Rosen, V. (2006). BMP2 activity, although dispensable for bone formation, is required for the initiation of fracture healing. *Nature Genetics*, 38(12), 1424–1429.
- Vescini, F., & Grimaldi, F. (2012). PTH 1-84: bone rebuilding as a target for the therapy of severe osteoporosis. *Clinical Cases in Mineral and Bone Metabolism*, 9(1), 31–36.

VITA

[REDACTED]
[REDACTED]
[REDACTED]
[REDACTED]
[REDACTED]

[REDACTED]

- [REDACTED]
- [REDACTED]

[REDACTED]

- [REDACTED]
[REDACTED]
[REDACTED]
[REDACTED]
[REDACTED]
[REDACTED]
[REDACTED]
[REDACTED]
[REDACTED]
[REDACTED]
[REDACTED]

- [REDACTED]
[REDACTED]
[REDACTED]
[REDACTED]
[REDACTED]
[REDACTED]
[REDACTED]
[REDACTED]
[REDACTED]

- [REDACTED]
[REDACTED]
[REDACTED]
[REDACTED]
[REDACTED]
[REDACTED]

[REDACTED]

[REDACTED]

- [REDACTED]

- [REDACTED]

- [REDACTED]

[REDACTED]

[REDACTED]

- [REDACTED]

- [REDACTED]